ELSEVIER

Preparation, structural study from neutron diffraction data and magnetism of the disordered perovskite Ca(Cr$_{0.5}$Mo$_{0.5}$)O$_3$

M.J. Martínez-Lope[a], J.A. Alonso[a,*], M.T. Casais[a], M. García-Hernández[a], V. Pomjakushin[b]

[a]Instituto de Ciencia de Materiales de Madrid, CSIC, Cantoblanco, 28049 Madrid, Spain
[b]Laboratory for Neutron Scattering, ETHZ & PSI, CH-5232 Villigen PSI, Switzerland

Abstract

We report on the preparation and characterization of the Ca(Cr$_{0.5}$Mo$_{0.5}$)O$_3$ perovskite, obtained in the search of the hypothetical double perovskite Ca$_2$CrMoO$_6$. This material was prepared in polycrystalline form by solid state reaction in H$_2$/Ar flow. It has been studied by X-ray and neutron powder diffraction (NPD) and magnetic measurements. Ca(Cr$_{0.5}$Mo$_{0.5}$)O$_3$ crystallizes in the orthorhombic Pbnm (No. 62) space group, with the unit-cell parameters $a = 5.4110$ (4) Å, $b = 5.4795$ (5) Å, $c = 7.6938$ (6) Å. There is a complete disordering of Cr^{3+} and Mo^{5+} over the B-site of the perovskite, and the (Cr,Mo)O$_6$ octahedra are tilted by 12.4° in order to optimize the Ca–O bond lengths. The magnetic susceptibility is characteristic of a ferrimagnetic behavior, with $T_C = 125$ K, and a small saturation magnetization at $T = 5$ K, of 0.05 μ_B/f.u.
© 2006 Elsevier Inc. All rights reserved.

Keywords: Perovskite structure; Anti-site disorder; Double perovskite; Ferrimagnetic behavior; Neutron diffraction

1. Introduction

Double perovskites $A_2B'B''O_6$ (where A = alkaline-earth or rare-earth and B' and B'' are transition metal ions), can be viewed as a regular arrangement of corner-sharing $B'O_6$ and $B''O_6$ octahedra, alternating along the three directions of the crystal, with the large A cations occupying the voids in between the octahedra. If the difference in charge of the B' and B'' cations is large, these ions assume an ordered arrangement in the perovskite lattice [1–5]. There has been a revival in the interest on double perovskites since the report of magnetoresistance (MR) properties in Sr$_2$FeMoO$_6$ [6–7]. This perovskite is a half-metallic ferrimagnet, with a Curie temperature significantly above RT, $T_C = 415$ K.

Moreover, the occurrence of MR properties has also been observed in other members of the $A_2B'B''O_6$ family. The A = Ca and Ba analogues of the A_2FeMoO$_6$ series were also found to exhibit semimetallic and ferrimagnetic

properties [8,9–11]. Double perovskites A_2FeReO$_6$ (A = Ba and Ca), also present [12] half metallic ground state with the ferrimagnetic coupling of Fe^{3+} and Re^{5+} and a relatively high Curie temperature T_C. On the other hand, MR properties have also been reported on Cr-based double perovskites for instance Sr$_2$CrMoO$_6$ which is ferrimagnetic ($T_C = 450$ K) although it shows considerable anti-site disorder [13], implying that a fraction of Cr^{3+} cations occupy Mo^{5+} positions and vice versa.

We have been interested in the hypothetical double perovskite Ca$_2$CrMoO$_6$. A material with this nominal composition was studied in the 1960s, and it was described as an orthorhombic perovskite showing a ferromagnetic behavior below $T_C = 125$ K [14]. In the present work, we describe the synthesis of Ca$_2$CrMoO$_6$, prepared by solid state reaction in reducing conditions, and the results of a neutron powder diffraction (NPD) and magnetic study on a well-crystallized sample, demonstrating that there is a complete anti-site disorder over the B positions of the perovskite, in such a way that it should be reformulated as Ca(Cr$_{0.5}$Mo$_{0.5}$)O$_3$.

*Corresponding author. Fax: +34 91 372 06 23.
E-mail address: ja.alonso@icmm.csic.es (J.A. Alonso).

2. Experimental

Ca_2CrMoO_6 perovskite was prepared by solid-state reaction, from stoichiometric amounts of analytical grade $CaCO_3$, $(NH_4)_6Mo_7O_{24} \cdot 4H_2O$ and $Cr(NO_3)_2 \cdot 6H_2O$. The reactants were mixed, ground and calcined at $900\,°C$ for 4 h in air. Afterwards, the resulting black powder was ground and treated in an H_2/Ar (1%/99%) flow at $1290\,°C$ for 12 h.

The initial characterization of the product was carried out by X-ray diffraction (XRD) (CuKα, $\lambda = 1.5406\,Å$). NPD data were collected at the high resolution HRPT diffractometer [15] of the SINQ spallation source, at the Paul Scherrer Institute, Villigen, Switzerland. The patttern was collected at room temperature (RT) with a wavelength of $1.494\,Å$. The high intensity mode was used; the collection time was 2 h. The refinement of the crystal structure was performed by the Rietveld method, using the FULLPROF refinement program [16]. A pseudo-Voigt function was chosen to generate the line shape of the diffraction peaks. The following parameters were refined in the final run: scale factor, background coefficients, zero-point error, pseudo-Voigt corrected for asymmetry parameters, positional coordinates, isotropic thermal factors and occupancy factors for oxygen atoms. The coherent scattering lengths for Ca, Cr, Mo and O were 4.70, 3.635, 6.720 and 5.803 fm, respectively.

The magnetic measurements were performed in a commercial superconducting quantum interference device magnetometer (SQUID). The susceptibility was measured under a 1 kOe magnetic field and at the temperature interval $5 < T < 400\,K$. An isothermal magnetization curve was obtained for magnetic fields going from -50 to $50\,kOe$ at $T = 5\,K$.

3. Results and discussion

Ca_2CrMoO_6 was obtained as a black well-crystallized powder. The preparation temperature resulted to be rather critical to maximize the yield of perovskite phase; thermal treatments below $1290\,°C$ led to mixtures with $CaMoO_4$, whereas above this temperature a competitive $CaCr_2O_4$ phase stabilizes. The XRD diagram of the final product is shown in Fig. 1. The pattern is characteristic of a perovskite-type structure, and shows no superstructure peaks corresponding to the long-range Cr/Mo ordering. Minor amounts of $CaCr_2O_4$ were detected from either XRD or NPD data; the most intense peaks from the impurity are indicated with stars in Fig. 1.

The crystal structure refinement was performed from high-resolution NPD data collected at RT with a wavelength $\lambda = 1.494\,Å$. In a first trial, the crystal structure was defined considering the structural model described for Ca_2FeMoO_6 [17]. This model corresponds to an ordered double perovskite where Fe and Mo occupy different crystallographic sites, with distinct oxygen environments. It is defined in the monoclinic $P2_1/n$ space group
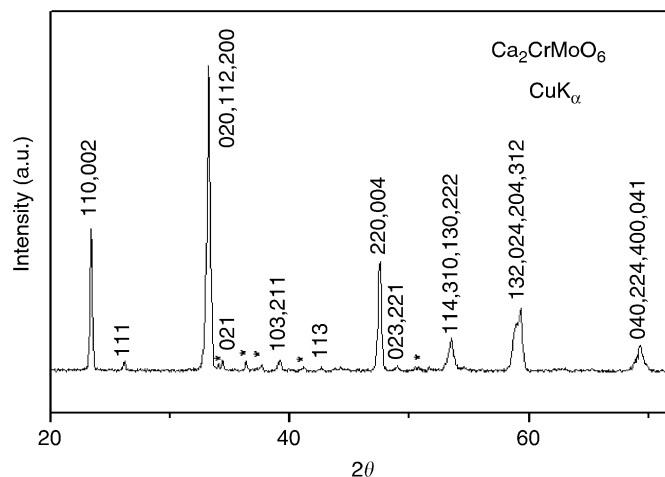

Fig. 1. XRD pattern for $Ca(Cr_{0.5}Mo_{0.5})O_3$, indexed in an orthorhombic unit cell with $a = 5.4110\,(4)\,Å$, $b = 5.4795\,(5)\,Å$, $c = 7.6938\,(6)\,Å$.

where, besides the two crystallographically independent B positions (Fe and Mo), there are 3 kinds of non-equivalent oxygen atoms (O1, O2 and O3), all in general (x, y, z) positions. The details of the atomic positions for Ca_2FeMoO_6 can be found elsewhere [17]. The refinement of the Ca_2CrMoO_6 structure in this monoclinic model led to a reasonable reliability factor of $R_I = 5.5\%$. The monoclinic β angle was virtually equal to $90°$, $\sim89.99°$. Moreover, the refinements of the level of anti-site defects (Cr at Mo sites, and vice versa) gave rise to an almost random distribution of both kinds of atoms over the B positions. This trial refinement gave full support to the idea that the hypothetical "double" perovskite Ca_2CrMoO_6 is in fact an almost fully disordered perovskite whose formula should be rewritten as $Ca(Cr_{0.5}Mo_{0.5})O_3$. This result is in agreement with the general observation that charge differences $\geqslant 3$ are required to obtain high degrees of charge ordering in double perovskites [18].

In consequence, in a second set of refinements the crystal structure was defined in the orthorhombic space group $Pbnm$ (No. 62), with unit-cell parameters related to a_0 (ideal cubic perovskite, $a_0 \approx 3.8\,Å$) as $a \approx b \approx \sqrt{2}a_0$, $c \approx 2a_0$ which corresponds to the $GdFeO_3$-type structure [19]. Ca atoms were located at $4c$ positions, Cr and Mo atoms where distributed at random at $4b$ sites and oxygen atoms at $4c$ and $8d$ positions, respectively. The oxygen stoichiometry at O1 and O2 positions was checked by refining their occupancy factors; no oxygen vacancies were detected within the standard deviations. $CaCr_2O_4$ was included as secondary phase in the refinement; this phase is orthorhombic, space group $Pbnm$ [20]. From the scale factors of the main and secondary phases, we estimated 1.77% in weight of $CaCr_2O_4$. The relative amount of Cr vs. Mo at B positions was also refined; a slight Cr deficiency was observed, in agreement with the presence of a Cr-rich impurity in the pattern; the final refined stoichiometry is $Ca(Cr_{0.44(2)}Mo_{0.56(2)})O_{2.98(2)}$. A good fit between the

observed and the calculated profiles was obtained, as shown in Fig. 2. The final reliability factor dropped to $R_I = 3.30\%$. The final lattice parameters were $a = 5.4110$ (4) Å, $b = 5.4795$ (5) Å, $c = 7.6938$ (6) Å and $V = 228.12$ (3) Å^3. Table 1 lists the structural and thermal parameters, together with unit-cell parameters refined from NPD data at RT.

The mean interatomic distances and some selected bond angles are listed in Table 2. A view of the crystal structure of $Ca(Cr_{0.5}Mo_{0.5})O_3$ is shown in Fig. 3. It is fairly distorted due to the small size of Ca^{2+} cations, which force the $(Cr,Mo)O_6$ octahedra to tilt in order to optimize the Ca–O bond distances. The average tilting angle can be estimated as $\phi = (180-\theta)/2$, where $\theta = \langle(Cr,Mo)-O-(Cr,Mo)\rangle = 155.20°$, then $\phi = 12.4°$.

As shown in Table 2, Ca–O distances range from 2.366 to 3.081 Å; the effective coordination of Ca^{2+} cations can be considered as eightfold, only considering the bond-lengths below 2.662 Å, with an average $\langle Ca-O\rangle_{8short}$ value 2.526 Å which compares well that expected from the ionic radii sums [21] of 2.52 Å for $^{VIII}Ca^{2+}$ (i.r.: 1.12 Å) and $^{VI}O^{2-}$ (i.r.: 1.40 Å). For the $(Cr,Mo)-O$ bonds the average distance of 1.972 Å is somewhat shorter than the expected of 2.01 Å for $(^{VI}Cr^{3+}, ^{VI}Mo^{5+})$ ions (i.r.: (0.615, 0.61 Å).

The thermal evolution of the magnetic susceptibility for $Ca(Cr_{0.5}Mo_{0.5})O_3$ is displayed in Fig. 4a. There is a notable increase of the susceptibility below $T_C = 125$ K, which tends to saturation at lower temperatures. The reciprocal susceptibility (right axis of Fig. 4a), exhibits a significant curvature at temperatures immediately above T_C, followed by an anomaly at about 350 K, and presents a linear behavior only in a small temperature interval, above 350 K. This anomaly could correspond to the onset of short-range magnetic ordering, perhaps in minority regions exhibiting some *B*-site cationic ordering, in this globally disordered sample. A Curie–Weiss fit in the 350–400 K temperature range from the inverse of the susceptibility curve yields a paramagnetic temperature $\theta_P = -33(1)$ K and an effective paramagnetic moment of 3.83(1) μ_B. For $Ca(Cr_{0.5}Mo_{0.5})O_3$ with the electronic configuration $Cr^{3+}(3d^3)-Mo^{5+}(4d^1)$, the theoretical effective magnetic moment (spin only) is 4.24 μ_B/f.u., in reasonable agreement with the experimental value. The mentioned impurity of stoichiometry $CaCr_2O_4$ has been reported to undergo antiferromagnetic ordering below $T_N = 80$ K [22,23]; in the susceptibility vs. T curve (Fig. 4) it is not possible to detect any anomaly at this temperature, probably because of the small fraction of this impurity phase present in the sample. We can assume that the $CaCr_2O_4$ impurity has no influence on the global magnetic properties of the perovskite.

The isothermal magnetization curve of $Ca(Cr_{0.5}Mo_{0.5})O_3$ measured at $T = 5$ K is shown in Fig. 4b. The
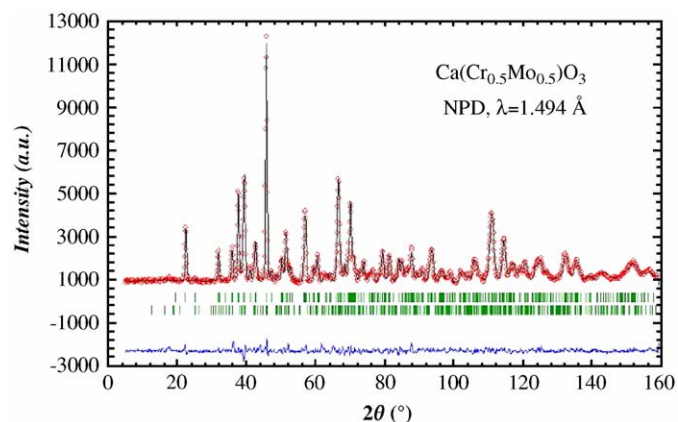

Fig. 2. Observed (circles) calculated (full line), and difference (bottom) NPD Rietveld profiles for stoichiometric $Ca(Cr_{0.5}Mo_{0.5})O_3$ at 295 K. The second series of tick marks correspond to the Bragg reflections of the $CaCr_2O_4$ impurity phase.

Table 2
Main interatomic distances (Å) and angles (deg) for $Ca(Cr_{0.5}Mo_{0.5})O_3$

(Cr,Mo)–O1 (*x2*)	1.9648(9)
(Cr,Mo)–O2 (*x2*)	1.968 (3)
(Cr,Mo)–O2 (*x2*)	1.984 (3)
$\langle(Cr,Mo)-O\rangle$	1.972 (2)
(Cr,Mo)–O1–(Cr,Mo)	156.46 (4)
(Cr,Mo)–O2–(Cr,Mo) (*x2*)	154.0 (1)
$\langle(Cr,Mo)-O-(Cr,Mo)\rangle$	155.20 (7)
Ca–O1	3.077 (5)
Ca–O1	2.467 (5)
Ca–O1	3.081 (8)
Ca–O1	2.365 (8)
Ca–O2 (*x2*)	2.648 (6)
Ca–O2 (*x2*)	2.379 (5)
Ca–O2 (*x2*)	2.662 (4)
$\langle Ca-O\rangle_{8short}$	2.526 (5)

Table 1
Structural parameters for $Ca(Cr_{0.44}Mo_{0.56})O_3$ refined in the orthorhombic *Pbnm* space group at room temperature from NPD data

Atom	Site	x	y	z	f_{occ}	B (Å^2)
Ca	4c	0.994 (1)	0.0393 (7)	1/4	1.0	1.28 (8)
Cr	4b	1/2	0	0	0.44 (2)	0.35 (6)
Mo	4b	1/2	0	0	0.56 (2)	0.35 (6)
O1	4c	0.0720 (8)	0.4829 (6)	1/4	1.00 (2)	0.59 (10)
O2	8d	0.7053 (5)	0.2915 (5)	0.0385 (4)	0.99 (1)	0.79 (7)

Lattice parameters: $a = 5.4110$ (4) Å, $b = 5.4795$ (5) Å, $c = 7.6938$ (6) Å and $V = 228.12$ (3) Å^3.
Discrepancy factors: $\chi^2 = 4.06$, $R_p = 3.92\%$, $R_{wp} = 5.21\%$, $R_{exp} = 2.59\%$ and $R_{Bragg} = 3.30\%$.

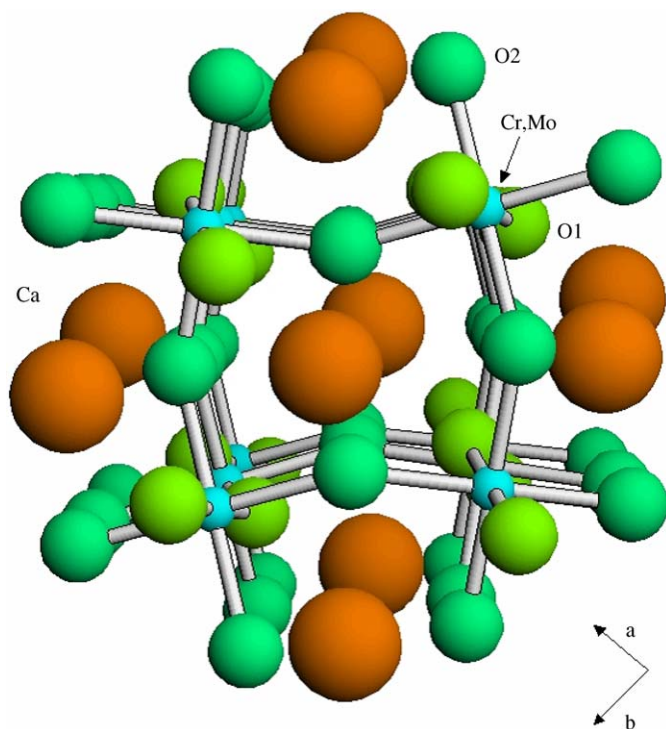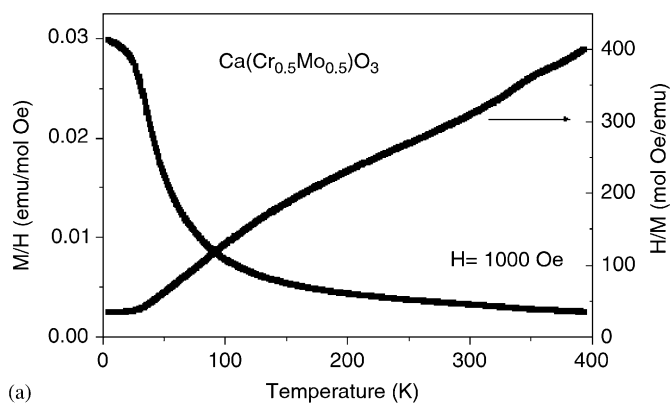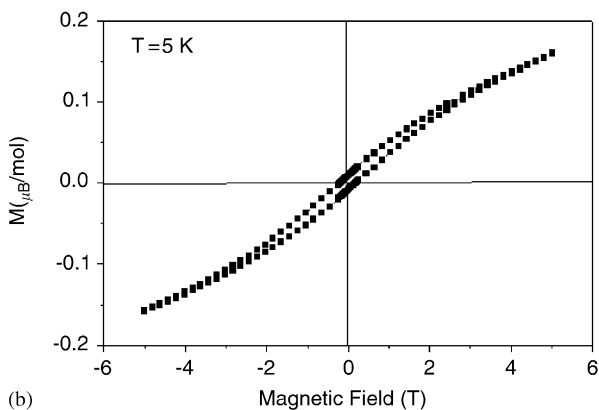Fig. 3. Schematic representation of the crystal structure of $Ca(Cr_{0.5}Mo_{0.5})O_3$ showing the tilting of the $(Cr_{0.5}Mo_{0.5})O_6$ octahedra. Large spheres represent Ca atoms.

Fig. 4. (a) Temperature dependence of the magnetic susceptibility and reciprocal susceptibility of $Ca(Cr_{0.5}Mo_{0.5})O_3$. (b) Magnetization isotherm at 5 K.

presence of a hysteresis loop with a very small remnant magnetization, of around $0.05\,\mu_B$/formula, suggests the presence of a weak ferromagnetism phenomenon in $Ca(Cr_{0.5}Mo_{0.5})O_3$. For the maximum applied magnetic field of 5 T, the magnetization reaches a maximum value of $0.15\,\mu_B$/formula, although it is far from saturation. These features are reminiscent to those previously reported for Ca_2CrMoO_6 [14], describing this perovskite as a ferromagnet with a T_C of 125 K.

It is worth discussing the magnetic properties of $Ca(Cr_{0.5}Mo_{0.5})O_3$ compared with those of the double perovskite Sr_2FeMoO_6. In a simple picture, its ferrimagnetic structure can be described as an ordered array of parallel Fe^{3+} $(S = 5/2)$ magnetic moments, antiferromagnetically coupled with Mo^{5+} $(S = 1/2)$ spins. In this ideal model, the saturation magnetization, at low temperature, would be of $4\,\mu_B$ per formula unit (f.u.). In the real world, such a large magnetization value has not been obtained for bulk Sr_2FeMoO_6 up to date; instead smaller values below $3.7\,\mu_B$/f.u. have been reported [6,24,25]. The origin of this difference with the theoretical magnetization can be found in the anti-site B-cation disorder, implying that some Mo^{5+} cations occupy the positions of Fe^{3+} cations, and viceversa. This effect can be dramatically increased in samples prepared at low temperatures, where the amounts of anti-site defects can overcome 80% [26]. For a highly disordered sample of Sr_2FeMoO_6 [26], a saturation magnetization as low as $0.8\,\mu_B$/f.u. for $H = 5\,T$ was reported. In an hypothetically 100% ordered Ca_2CrMoO_6 perovskite, a saturation magnetization of $2\,\mu_B$/f.u. would be expected for a perfect ferrimagnetic long distance ordering of Cr^{3+} $(S = 3/2)$ and Mo^{5+} $(S = 1/2)$. The observed reduction in magnetization is concomitant with the high degree of anti-site disordering observed in this sample. The almost random distribution of Cr/Mo cations implies that the Cr–O–Cr configuration frequently occur (as well as Mo–O–Mo configurations); in these regions we must consider that the Cr–O–Cr magnetic interactions are similar to those happening in $LaCrO_3$ perovskite, which experiences an AFM ordering below a surprisingly high Néel temperature, $T_N = 282\,K$ [27]. Our reciprocal susceptibility curve (Fig. 4a, right axis) show a convex curvature above T_C followed by a broad concavity in the 250–300 K interval, and the Curie–Weiss fit gives a negative Weiss temperature which also suggests the presence of AFM interactions.

Our picture shows a disordered Cr/Mo pattern in which the Cr–O–Cr superexchange AFM interactions are comparable to those existing in $LaCrO_3$; the coupling between near-neighbor Cr–Cr, Cr–Mo or Mo–Mo atoms is always AFM. In a perfectly disordered system, consisting of a random distribution of Cr and Mo cations, there are statistically occurring patches of Cr of several atoms (5–10 or more), all of them coupled AFM (the same for Mo) and the different patches are also coherently connected by the atoms in between. In overall, there is total

cancellation of the moments of both kinds of atoms and the expected saturation magnetization would equal zero; our observation of a small value implies that there is some residual degree of ordering, giving rise to a small unbalance between the up-spin and down spin Cr^{3+} sublattices. We can estimate the saturation magnetization of the Cr^{3+}/Mo^{5+} ferrimagnetic system as $Ms = (2-2x)\,\mu_B$/f.u., where x is the degree of disordering. For a saturation magnetization $0.05\,\mu_B$/f.u., we can evaluate a degree of disordering of 97.5%. This justifies our assumption that this compound can be considered as a fully disordered perovskite from the structural point of view.

4. Conclusions

$Ca(Cr_{0.5}Mo_{0.5})O_3$ is an almost fully *B*-site disordered perovskite showing a $GdFeO_3$-type structure, consisting of a network of strongly tilted $(Cr,Mo)O_6$ corner-sharing octahedra, with average tilting angles of 12.4°. The magnetic properties correspond to a weak ferromagnet with a low saturation magnetization of $0.05\,\mu_B$/f.u. A fit to the Curie–Weiss law in the paramagnetic region confirms the electronic configurations $Cr^{3+}(3d^3)$–$Mo^{5+}(4d^1)$. Given the random distribution of Cr and Mo over the *B* positions of the perovskite, it is reasonable to think that near-neighbor Cr–Cr atoms are antiferromagnetically coupled, by virtue of strong superexchange Cr–O–Cr interactions, similar to those existing in the antiferromagnetic $LaCrO_3$ perovskite. The observed saturation magnetization at $T = 5\,K$ arises form an unbalance of the up and down Cr^{3+} spins, corresponding to a very weak level of long-range ordering at *B* positions, which can be estimated to be lower than 3%.

Acknowledgments

References

[1] E.J. Fresia, L. katz, R. Ward, J. Am. Chem. Soc. 81 (1959) 4783.
[2] A.W. Sieight, R. Ward, J. Am. Chem. Soc. 83 (1961) 1088.
[3] J. Longo, R. Ward, J. Am. Chem. Soc. 83 (1961) 2816.
[4] F. Galasso, Inorg. Chem. 2 (1963) 483.
[5] T. Nakamura, J.H. Choy, J. Solid State Chem. 20 (1977) 233.
[6] K.I. Kobayaski, T. Kimura, H. Sawada, K. Terakura, Y. Tokura, Nature 395 (1998) 677.
[7] T.H. Kim, M. Uehara, S. Lee, S.-W. Cheong, Appl. Phys. Lett. 74 (1999) 1731.
[8] A. Maignan, B. Raveau, C. Martin, M. Hervieu, J. Solid State Chem. 144 (1999) 224.
[9] J.A. Alonso, M.T. Casais, M.J. Martínez-Lope, P. Velasco, A. Muñoz, M.T. Fernández-Díaz, Chem. Mater. 12 (2000) 161.
[10] R.P. Borges, R.M. Thomas, C. Cullinan, J.M.D. Coey, R. Suryanarayan, L. Ben-Dor, L. Pinsard-Gaudart, A. Revcolevschi, J. Phys. Condens. Matter 11 (1999) L445.
[11] C. Ritter, M.R. Ibarra, L. Morellón, J. Blasco, J. García, J.M. De Teresa, J. Phys. Condens. Matter 12 (2000) 8295.
[12] W. Prellier, W. Smolyaniniva, A. Bisbas, C. Galley, R.L. Greene, K. Ramesha, J. Gopalakrishnan, J. Phys. Condens. Matter 12 (2000) 965.
[13] A. Arulraj, K. Ramesha, J. Gopalakrishnan, C.N.R.J. Rao, Solid State Chem. 155 (2000) 233.
[14] F.K. Patterson, C.W. Moeller, R. Ward, Inorg. Chem. 2 (1963) 196.
[15] P. Fischer, G. Frey, M. Koch, M. Koennecke, V. Pomjakushin, J. Schefer, R. Thut, N. Schlumpf, R. Buerge, U. Greuter, S. Bondt, E. Berruyer, Physica B 46 (2000) 276.
[16] J. Rodríguez-Carvajal, Physica B (Amsterdam) 192 (1993) 55.
[17] J.A. Alonso, M.T. Casais, M.J. Martínez-Lope, J.L. Martínez, P. Velasco, A. Muñoz, M.T. Fernández-Díaz, Chem. Mater. 12 (2000) 161.
[18] M.T. Anderson, K.B. Greenwood, G.A. Taylor, K.R. Poeppelmeier, Prog. Solid State Chem. 22 (1993) 197.
[19] S. Geller, J. Chem. Phys. 24 (1956) 1236.
[20] W. Hoerkner, Hk. Mueller-Buschbaum, Z. Naturforch. B 2 (1977) 1947.
[21] R.D. Shannon, Acta Crystallogr. A 32 (1976) 751.
[22] M.M. Schieber, Experimental Magnetochenistry, Nonmetallic Magnetic Materials, North-Holland, Amsterdam, 1967 (p. 265).
[23] L.M. Corliss, J.M. Hastings, W. Kunnmann, Phys. Rev. 160 (1967) 408.
[24] Y. Tomioka, T. Okuda, Y. Okimoto, R. Kumai, K.-I. Kobayashi, Y. Tokura, Phys. Rev. B 61 (2000) 422.
[25] Ll. Balcells, J. Navarro, M. Bibes, A. Roig, B. Martínez, J. Fontcuberta, Appl. Phys. Lett. 78 (2001) 781.
[26] D. Sánchez, J.A. Alonso, M. García-Hernández, M.J. Martínez-Lope, M.T. Casais, J.L. Martínez, J. Mater. Chem. 13 (2003) 1771.
[27] R. Aleonard, R. Pauthenet, J.P. Rebouillat, C. Veyret, J. Appl. Phys. 39 (1968) 379.